The Journal of Infectious Diseases

MAJOR ARTICLE

Middle East Respiratory Syndrome Coronavirus Efficiently Infects Human Primary T Lymphocytes and Activates the Extrinsic and Intrinsic Apoptosis Pathways

Hin Chu,[1,2,3,4] Jie Zhou,[1,2,3,4] Bosco Ho-Yin Wong,[2] Cun Li,[2] Jasper Fuk-Woo Chan,[1,2,3,4] Zhong-Shan Cheng,[2] Dong Yang,[2] Dong Wang,[2] Andrew Chak-Yiu Lee,[2] Chuangen Li,[2] Man-Lung Yeung,[1,2,3,4] Jian-Piao Cai,[2] Ivy Hau-Yee Chan,[5] Wai-Kuen Ho,[5] Kelvin Kai-Wang To,[1,2,3,4] Bo-Jian Zheng,[1,2,3,4] Yanfeng Yao,[6] Chuan Qin,[6] and Kwok-Yung Yuen[1,2,3,4,7]

[1]State Key Laboratory of Emerging Infectious Diseases, [2]Department of Microbiology, [3]Research Centre of Infection and Immunology, [4]Carol Yu Centre for Infection, [5]Department of Surgery, University of Hong Kong, Hong Kong Special Administrative Region, [6]Institute of Laboratory Animal Sciences, Chinese Academy of Medical Sciences, and [7]Collaborative Innovation Center for Diagnosis and Treatment of Infectious Diseases, Zhejiang University, China

(See the editorial commentary by Ying, Li, and Dimitrov on pages 877–9.)

Middle East respiratory syndrome (MERS) is associated with a mortality rate of >35%. We previously showed that MERS coronavirus (MERS-CoV) could infect human macrophages and dendritic cells and induce cytokine dysregulation. Here, we further investigated the interplay between human primary T cells and MERS-CoV in disease pathogenesis. Importantly, our results suggested that MERS-CoV efficiently infected T cells from the peripheral blood and from human lymphoid organs, including the spleen and the tonsil. We further demonstrated that MERS-CoV infection induced apoptosis in T cells, which involved the activation of both the extrinsic and intrinsic apoptosis pathways. Remarkably, immunostaining of spleen sections from MERS-CoV–infected common marmosets demonstrated the presence of viral nucleoprotein in their $CD3^+$ T cells. Overall, our results suggested that the unusual capacity of MERS-CoV to infect T cells and induce apoptosis might partly contribute to the high pathogenicity of the virus.

Keywords. MERS-CoV; T lymphocytes; apoptosis; caspase; tonsil; spleen; marmosets.

Middle East respiratory syndrome coronavirus (MERS-CoV) is a novel zoonotic betacoronavirus that causes severe acute respiratory syndrome (SARS)–like disease with extrapulmonary manifestations [1–3]. Despite the high resemblance between MERS and SARS, the case-fatality rate of MERS is >30%, which is 3 times than that of SARS [4–6]. Moreover, severe lymphopenia, which is an important prognostic factor for SARS, is commonly observed in patients with MERS [7, 8]. The high pathogenicity of MERS-CoV is partly explained by the MERS-CoV receptor dipeptidyl peptidase 4 (DPP4), which is abundantly found in most host cells [9, 10]. In in vitro and ex vivo studies, MERS-CoV exhibits broad tissue tropism that is unparalleled by other coronaviruses [11–14]. Upon entry, MERS-CoV efficiently evades the host innate immune response by the viral accessory proteins 4a, 4b, and 5, by papain-like protease, and by membrane (M) protein, which are potent interferon antagonists, and by downregulating the expression of genes within the antigen presentation pathway [15–21]. Moreover, we have previously demonstrated that MERS-CoV causes productive infection of monocyte-derived macrophages (MDMs) and monocyte-derived dendritic cells (MoDCs), the key professional antigen-presenting cells, which may facilitate systemic virus dissemination [14, 22]. Finally, MERS-CoV induces an aberrant cytokine/chemokine response that may be responsible for the cytokine dysregulation in severe MERS cases [14, 22, 23].

Intriguingly, DPP4 is recognized as an activation marker on T cells and plays pivotal roles in T-cell functions, including activation [24], signal transduction [25], and costimulation [26]. We postulate that the abundant expression of DPP4 on T cells may render the cells highly susceptible to MERS-CoV infection. Importantly, a recent study demonstrated that infection of DPP4-transduced T-cell–deficient mice with MERS-CoV resulted in the persistence of MERS-CoV in the lungs, while virus was cleared in control and B-cell–deficient mice [27]. These findings suggested that T cells might play crucial roles in the pathogenesis of MERS-CoV. In this study, we showed that MERS-CoV was capable of efficiently infecting human T cells from the peripheral blood, spleen, and tonsil. Moreover, MERS-CoV could infect the T cells in the spleen of common marmosets. Importantly, MERS-CoV infection in T cells induced massive apoptosis involving activation of both the extrinsic and intrinsic apoptosis pathways, which might be important in the pathogenesis of MERS.

MATERIALS AND METHODS

Preparation of Peripheral Blood Mononuclear Cells (PBMCs), T Cells, and Spleen- and Tonsil- Disassociated Cells

PBMCs and T cells were prepared as preciously described [28]. Tonsil- and spleen-disassociated cells were obtained

Received 29 April 2015; accepted 1 June 2015; published online 22 July 2015.

Correspondence: K.-Y. Yuen, Carol Yu Centre for Infection, Department of Microbiology, University of Hong Kong, Queen Mary Hospital, 102 Pokfulam Rd, Pokfulam, Hong Kong Special Administrative Region, China (kyyuen@hku.hk).

The Journal of Infectious Diseases® 2016;213:904–14

 DOI: 10.1093/infdis/jiv380

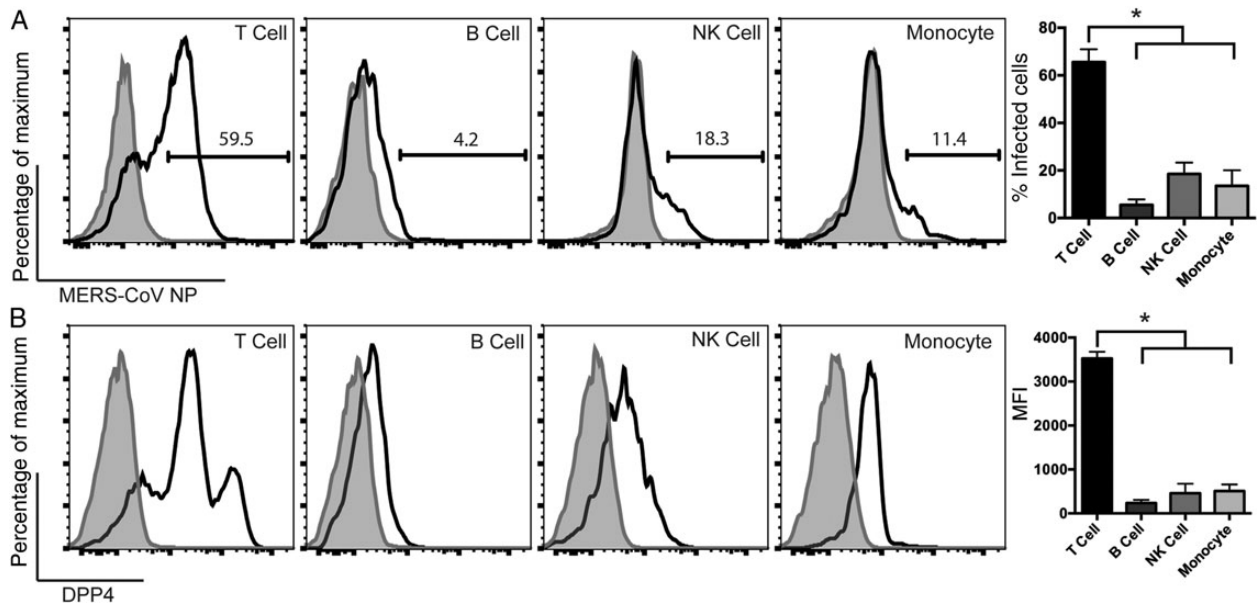

Figure 1. Middle East respiratory syndrome coronavirus (MERS-CoV) differentially infects subsets of human peripheral blood mononuclear cells (PBMCs). *A*, Human PBMCs were infected with MERS-CoV at 2 50% tissue culture infective doses per cell. At 24 hours after infection, infected cells were fixed with 4% paraformaldehyde (PA) and immunolabeled for detection of cell surface markers and MERS-CoV nucleoprotein (NP). The shaded curve and the solid line represent MERS-CoV NP expression from mock-infected and MERS-CoV–infected cells, respectively. The summary panel at the right represents the average percentage of infected cells from 3 different donors. *B*, Uninfected human PBMCs were fixed with 4% PA and immunolabeled for detection of surface DPP4 expression. The shaded curve and the solid line represented isotype and DPP4-specific staining, respectively. The summary panel at the right represents the average mean fluorescent intensity (MFI) from 3 different donors. In all panels, bars and error bars represented means and standard deviations, respectively. Statistical analyses were performed using the Student *t* test. $*P < .001$. Abbreviation: NK, natural killer.

from individuals undergoing splenectomy and tonsillectomy; all individuals provided written consent before cells were collected. Details are presented in the Supplementary Materials.

Infection of Common Marmosets

Approval by the institutional animal care and use committee was obtained for animal experiments [29]. Common marmosets were inoculated with 5×10^6 50% tissue culture infective doses ($TCID_{50}$) MERS-CoV intratracheally in 500 μL of Dulbecco's modified Eagle's medium. Organ samples were collected on necropsy as described previously [29–31].

Antibodies

Cell surface markers were obtained from BD Pharmingen, BioLegend, and Abcam. DPP4 antibody was obtained from R&D Systems. Immunostaining of MERS-CoV [14, 22] and SARS-CoV nucleoprotein (NP) [32] were performed as previously described.

Virus and Infections

MERS-CoV strain EMC/2012 (passage 8) was provided by Dr Ron Fouchier (Erasmus Medical Center) [1, 33]. MERS-CoV and SARS-CoV were cultured from Vero E6 cells. For infections, cells were inoculated with MERS-CoV or SARS-CoV at 2 $TCID_{50}$ per cell for 1 hour at 37°C.

Reverse Transcription–Quantitative Polymerase Chain Reaction (RT-qPCR)

RNA extraction and RT-qPCR were performed as previously described [14, 22, 34].

Terminal Deoxynucleotidyl Transferase dUTP Nick End Labeling (TUNEL) Assays

The TUNEL assay kit was purchased from Life Technologies. Labeling procedures were performed following protocols recommended by the manufacturer.

Active Caspase Assays

Active caspase 3 antibody was obtained from BD Pharmingen. CaspGLOW fluorescein active caspase 8 and 9 staining kits were obtained from eBioscience. Labeling was performed according to the manufacturer's protocol and is outlined in the Supplementary Materials.

Flow Cytometry

Immunostaining for flow cytometry was performed following standard procedures. Flow cytometry was performed using BD FACSCanto II (BD Biosciences), and data were analyzed using FlowJo vX (Tree Star).

Confocal Imaging of Marmoset Spleen Sections

MERS-CoV NP was labeled with guinea pig anti-MERS-CoV NP serum as mentioned above. $CD3^+$ T cells were identified with a mouse anti-human antibody (clone SP34-2) from BD

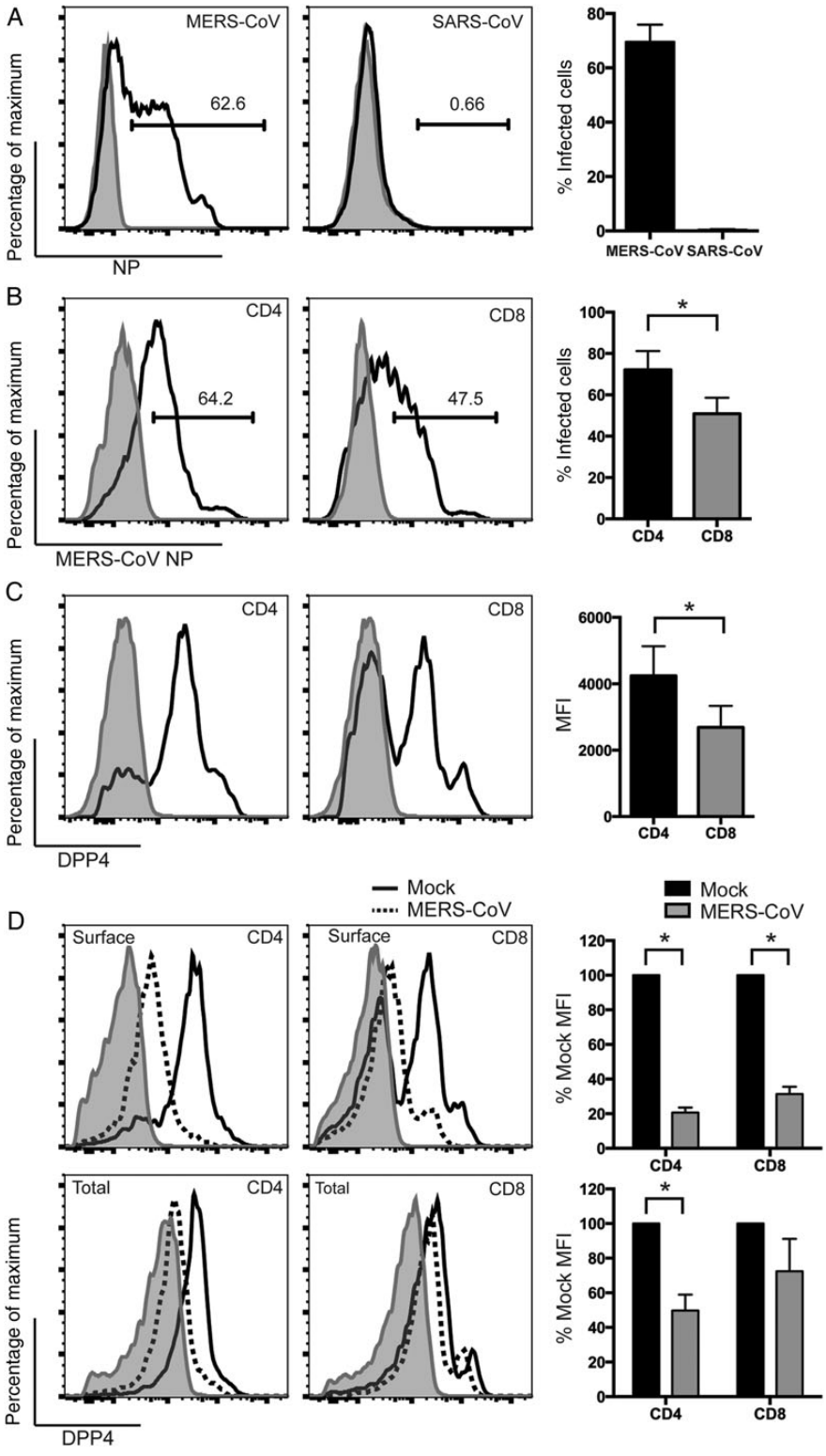

Figure 2. Middle East respiratory syndrome coronavirus (MERS-CoV) efficiently infects $CD4^+$ and $CD8^+$ T cells and downregulates surface dipeptidyl peptidase 4 (DPP4) in the infected cells. *A*, T cells were infected with MERS-CoV and severe acute respiratory syndrome CoV (SARS-CoV) at 2 50% tissue culture infective doses ($TCID_{50}$) per cell. Cells were fixed at 24 hours after infection and immunolabeled for detection of expression of MERS-CoV NP or SARS-CoV NP. The shaded curve and the solid line represent virus NP expression from mock-infected and MERS/SARS-CoV–infected cells, respectively. *B*, T cells were infected with MERS-CoV at 2 $TCID_{50}$ per cell. Cells were fixed at 24 hours after infection and immunolabeled for detection of CD4 or CD8 and MERS-CoV NP expression. The shaded curve and the solid line represent NP expression from mock-infected and MERS-CoV–infected cells, respectively. *C*, Uninfected T cells were fixed and immunolabeled for detection of CD4 or CD8 and surface DPP4 expression. The shaded curve and the solid line represent isotype and DPP4-specific staining, respectively. *D*, T cells were infected with MERS-CoV at 2 $TCID_{50}$ per cell. Cells were fixed at 24 hours after infection and immunolabeled for detection of CD4 or CD8, DPP4, and MERS-CoV NP expression. Surface or total DPP4 was detected by labeling the cells with the DPP4

Pharmingen. Images were acquired with a Carl Zeiss LSM 780 system.

Statistical Analysis

Statistical comparison was performed by the Student *t* test, using GraphPad Prism 6.

RESULTS

MERS-CoV Differentially Infects Subsets of Human PBMCs, and the Infectivity Correlates With Surface DPP4 Expressions

We hypothesized that T cells were potential targets of MERS-CoV infection. To test our hypothesis, we inoculated PBMCs with MERS-CoV and evaluated the proportion of MERS-CoV–infected T cells, B cells, natural killer (NK) cells, and monocytes with flow cytometry. Notably, a substantial proportion of T cells were infected by MERS-CoV. In contrast, MERS-CoV only modestly infected monocytes and NK cells, whereas it marginally infected B cells (Figure 1*A*). Quantitatively, the average percentages (±standard deviation [SD]) of MERS-CoV NP–positive T cells, B cells, NK cells, and monocytes were 65.6% ± 5.4%, 5.4% ± 2.4%, 18.5% ± 4.8%, and 13.5% ± 6.6%, respectively (Figure 1*A*). As expected, the percentage of MERS-CoV infection was in direct accordance with the level of surface DPP4 expression on these PBMC subsets (Figure 1*B*). Overall, we showed that MERS-CoV was capable of infecting T cells, NK cells, monocytes, and, to a less extent, B cells. The efficiency of infection highly correlated with the level of surface DPP4 expression.

MERS-CoV Efficiently Infects $CD4^+$ and $CD8^+$ T Cells and Downregulates Surface DPP4 in the Infected Cells

To further characterize MERS-CoV infection in T cells, we first challenged purified T cells with MERS-CoV and SARS-CoV and checked for NP expression. Strikingly, whereas a substantial number of T cells were infected by MERS-CoV, they were largely refractory to SARS-CoV infection (Figure 2*A*). This differential susceptibility might be in part attributed to the discrepancy in the expression levels of DPP4 and angiotensin converting enzyme 2 in T cells (Supplementary Figure 1). Next, we asked whether the 2 major populations of T cells, $CD4^+$ and $CD8^+$ T cells, were equally susceptible to MERS-CoV infection. As shown in Figure 2*B*, substantial numbers of both populations were infected by MERS-CoV. However, a significantly higher proportion of $CD4^+$ T cells (mean ± SD, 72.1% ± 9.1%) were infected, compared with $CD8^+$ cells (50.9% ± 7.7%). The degree of infection again correlated with surface DPP4 expression (Figure 2*C*). Next, because DPP4 plays essential roles in a broad array of T-cell functions [24–26], we evaluated the expression level of surface and total DPP4 on $CD4^+$ or $CD8^+$ T cells after MERS-CoV infection. Remarkably, MERS-CoV significantly downregulated surface DPP4 in infected $CD4^+$ T cells by 80% and $CD8^+$ T cells by 70% (Figure 2*D*). Changes in the total DPP4 level were less dramatic, with values of 50% and 30% for $CD4^+$ and $CD8^+$ T cells, respectively (Figure 2*D*). In contrast to DPP4, surface or total levels of CD4 and CD8 were unaltered in infected T cells (Supplementary Figure 2). Together, our data demonstrated that MERS-CoV but not SARS-CoV efficiently infected T cells and significantly downregulated surface DPP4 in the infected cells.

MERS-CoV Infection of Human T Cells Is Abortive

To grasp a more comprehensive picture of the replication kinetic of MERS-CoV in T cells, we measured the genome copy number of MERS-CoV from samples harvested at different time points. In stark contrast to MDMs [14] and MoDCs [22], in which MERS-CoV infections are productive, T cells failed to support MERS-CoV replication (Supplementary Figure 3). The number of MERS-CoV genome copies in the cell lysates (Supplementary Figure 3*A*) and supernatants (Supplementary Figure 3*B*) of infected T cells remained largely steady over time. As expected, SARS-CoV similarly failed to replicate in T cells. Intriguingly, the number of intracellular MERS-CoV genome copies was 2–3 logs higher than that of SARS-CoV (Supplementary Figure 3*A*). Therefore, our findings supported the notion that MERS-CoV efficiently entered T cells, although the infection was not productive, whereas SARS-CoV failed to enter T cells.

MERS-CoV but Not SARS-CoV Induces Apoptosis in T Cells

MERS-CoV is known to cause cytopathology in a number of cell lines [35, 36]. To examine whether MERS-CoV infection induced cell death in T cells, we assessed TUNEL activity in MERS-CoV–infected T cells and compared the findings to those in SARS-CoV– or mock-infected T cells. TUNEL assays detect DNA fragmentation that results from apoptotic signaling cascades and identifies cells in the last phase of apoptosis [37]. We detected an increased number of TUNEL-positive cells in MERS-CoV–infected T cells at as early as 6 hours after infection, compared with SARS-CoV– or mock-infected T cells. At 24 and 48 hours after infection, significantly more TUNEL-positive cells were detected in MERS-CoV–infected T cells comparing with findings for the 2 other groups (Figure 3*A*). Quantitatively, the mean percentages (±SD) of TUNEL-positive T cells upon MERS-CoV infection were 8.2% ± 2.7%, 20.0% ± 7.8%, and 27.8% ± 9.7% at 6, 24, and 48 hours after infection, respectively (Figure 3*B*). Thus, we concluded that MERS-CoV but not SARS-CoV induced apoptosis in T cells.

Figure 2 continued. antibody before or after cell permeabilization, respectively. The shaded curve represents isotype staining of DPP4. The solid line and dotted line represent DPP4 staining from mock-infected and MERS-CoV–infected cells, respectively. The DPP4 mean fluorescence intensity (MFI) in infected cells was calculated on the basis of $CD4^+$/MERS-CoV NP–expressing or $CD8^+$/MERS-CoV NP–expressing double-positive T-cell data. The DPP4 MFI in mock-infected cells was calculated on the basis of $CD4^+$ or $CD8^+$ T-cell data. The summary panels at the right represent the average percentage of infected cells (*A* and *B*), MFI (*C*), or percentage of mock MFI (*D*) from 3 different donors. In all panels, bars and error bars represent means and standard deviations. Statistical analyses were performed using the Student *t* test. $^*P < .05$.

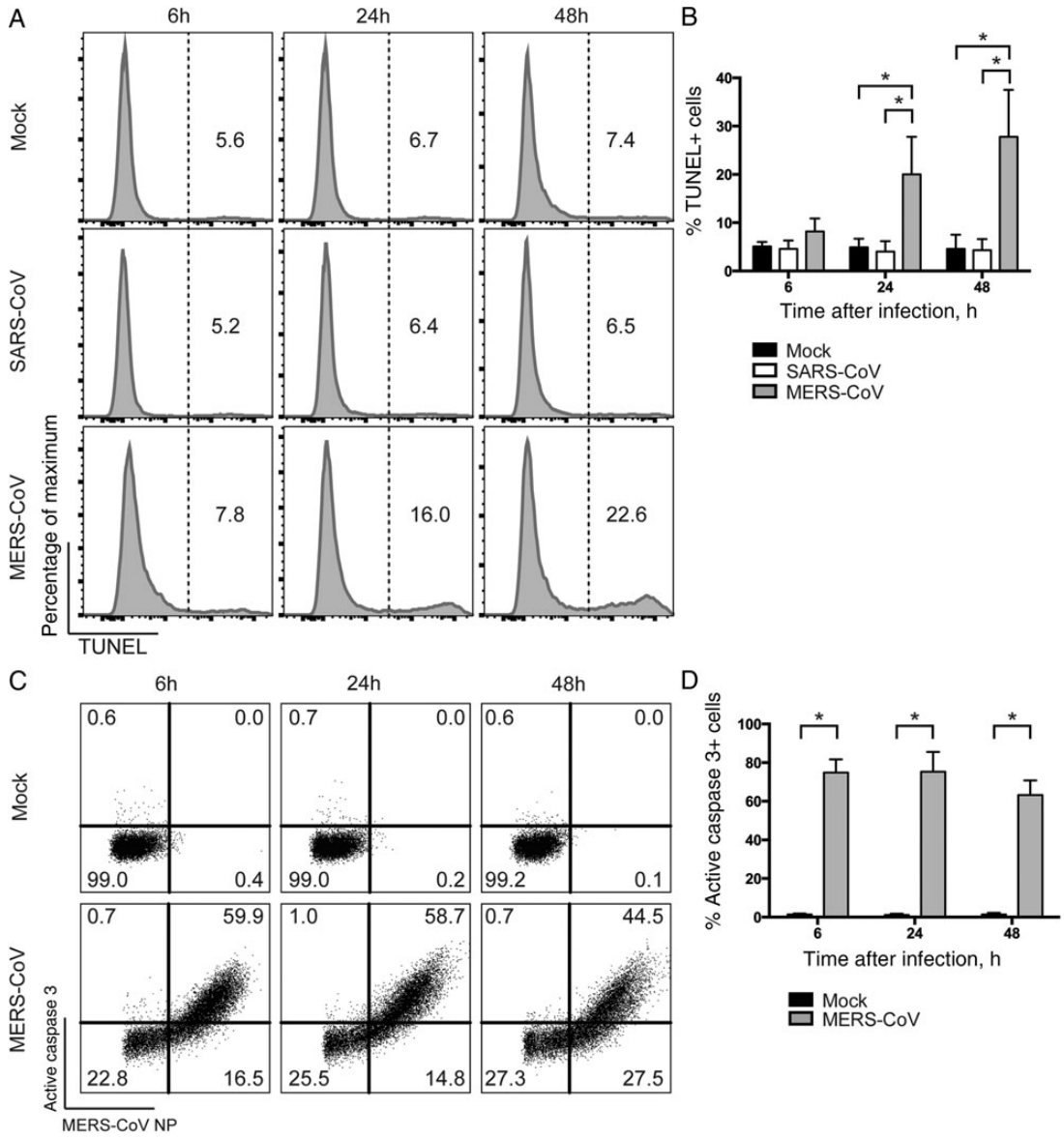

Figure 3. Middle East respiratory syndrome coronavirus (MERS-CoV) induces apoptosis and substantial upregulation of active caspase 3 in infected T cells. *A,* T cells were infected with MERS-CoV or severe acute respiratory syndrome CoV (SARS-CoV) at 2 50% tissue culture infective doses ($TCID_{50}$) per cell. Cells were fixed at the indicated time points and immunolabeled for detection of terminal deoxynucleotidyl transferase dUTP nick end labeling (TUNEL)–positive cells. *B,* The average percentage of TUNEL-positive cells from 3 different donors. *C,* T cells were infected with MERS-CoV at 2 $TCID_{50}$ per cell. Cells were fixed at the indicated time points and immunolabeled for detection of MERS-CoV nucleoprotein (NP) and active caspase 3. *D,* The average percentage of active caspase 3–positive cells among MERS-CoV NP^+ cells from 3 different donors. In all panels, bars and error bars represent means and standard deviations. Statistical analyses were performed using the Student *t* test. $^*P < .01$.

Apoptosis is a coordinated and energy-dependent process that can be triggered through the extrinsic (death receptor) or the intrinsic (mitochondrial) caspase-dependent pathways [38]. The 2 pathways end and converge at the execution phase, which involves the activation of execution caspases, including caspases 3, 6, and 7 [39]. Among them, caspase 3 is considered to be the most important executer caspase and is activated by any of the initiator caspases (caspases 2 and 8–10) [38]. Therefore, we evaluated the extent of caspase 3 activation in infected T cells. Remarkably, substantial active caspase 3 expression was evident in MERS-CoV–infected T cells as early as 6 hours after infection, and expression remained high over time (Figure 3*C*). Specifically, active caspase 3 was detected at a mean frequency (±SD) of 74.9% ±6.8%, 75.3% ± 10.2%, and 63.2% ± 7.6% among MERS-CoV-NP–positive T cells at 6, 24, and 48 hours after infection, respectively (Figure 3*D*). Caspase 3 activation was absent in mock-infected cells or in T cells that remained uninfected in the MERS-CoV–treated samples (Figure 3*C*). In summary, we demonstrated that caspase 3 was substantially activated in MERS-CoV–infected T cells early upon infection and remained highly expressed.

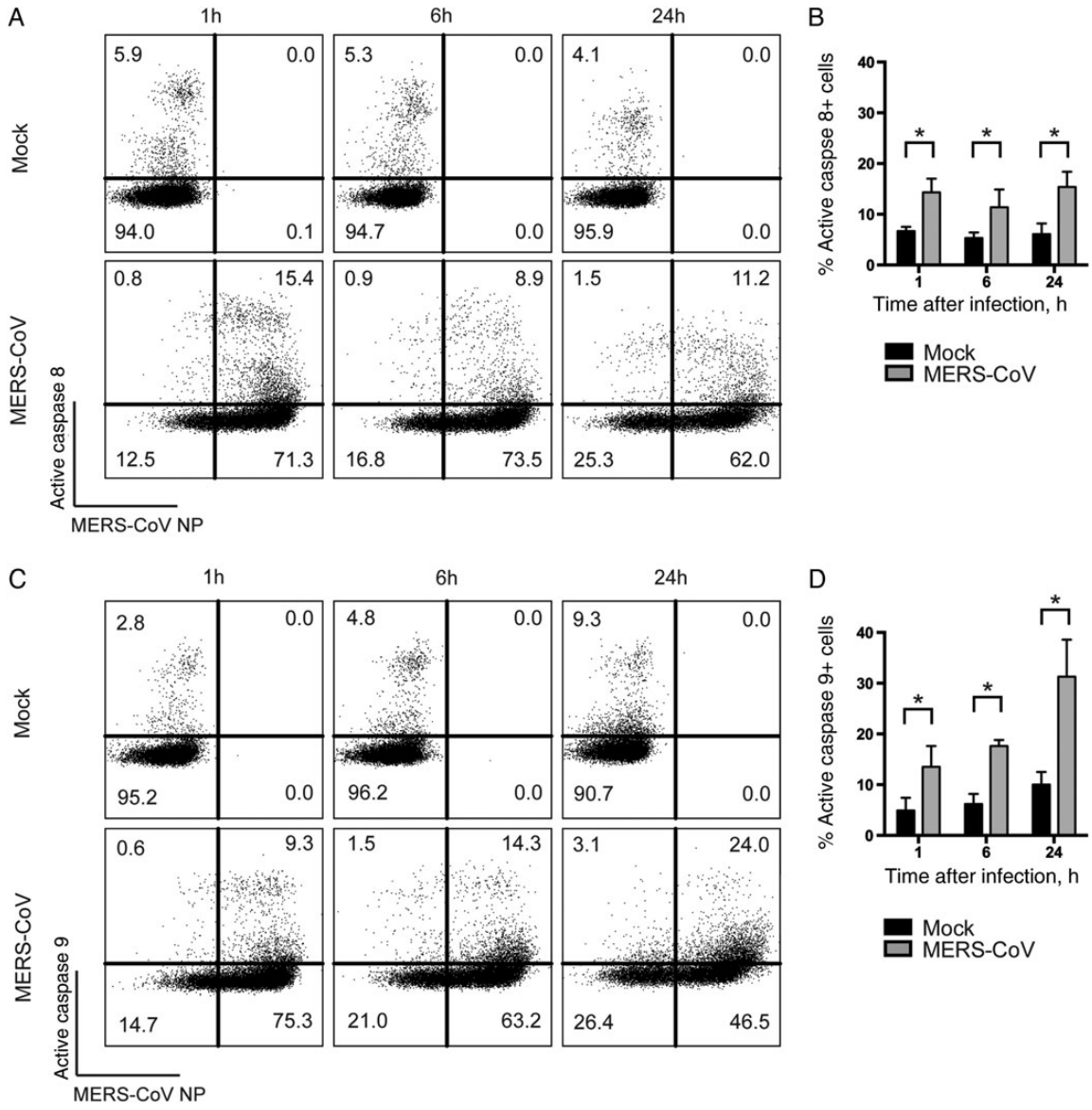

Figure 4. The extrinsic and intrinsic caspase-dependent apoptosis pathways are activated in Middle East respiratory syndrome coronavirus (MERS-CoV)–infected T cells. T cells were infected with MERS-CoV at 2 50% tissue culture infective doses per cell. At the indicated time points, infected cells were labeled with MERS-CoV nucleoprotein (NP), as well as FITC-IETD-FMK (for caspase 8; *A* and *B*) and FITC-LEHD-FMK (for caspase 9; *C* and *D*) for 1 hour at 37°C. The average percentage of active caspase 8–positive (*B*) or active caspase 9–positive (*D*) cells among MERS-CoV NP–expressing cells from 3 different donors was illustrated. In all panels, bars and error bars represent means and standard deviations. Statistical analyses were performed using the Student *t* test. $^*P < .05$.

Extrinsic and Intrinsic Caspase-Dependent Apoptosis Pathways Are Triggered in MERS-CoV–Infected T Cells

We then examined the degree of caspase 8 and caspase 9 activation, which represented the involvement of the extrinsic and intrinsic apoptosis pathway, respectively. Intriguingly, our results suggested that both caspase 8 and caspase 9 were activated starting as early as 1 hour after infection with MERS-CoV. The degree of caspase 8 activation in MERS-CoV–infected T cells was rather consistent over time (Figure 4*A*), with mean levels (±SD) of 14.3% ± 2.7%, 11.4% ± 4.8%, and 15.4% ± 3.0% at 1, 6, and 24 hours after infection, respectively (Figure 4*B*). An increasing level of caspase 9 activation was detected in MERS-CoV–infected T cells over time (Figure 4*C*). Specifically, the mean frequencies (±SD) of MERS-CoV–infected T cells expressing active caspase 9, at 1, 6, and 24 hours after infection were 13.5% ± 4.1%, 17.6% ± 1.2%, and 31.3% ± 7.3%, respectively (Figure 4*D*). Together, our results suggested that the extrinsic and intrinsic apoptosis pathways were triggered in MERS-CoV–infected T cells.

MERS-CoV–Induced Caspase 3 Activation in T Cells Occurs Rapidly Upon Infection and Is Not Inhibited by UV-Inactivated MERS-CoV

To compare the extent of MERS-CoV–induced cytopathology between cell lines and primary T cells, we infected Vero E6

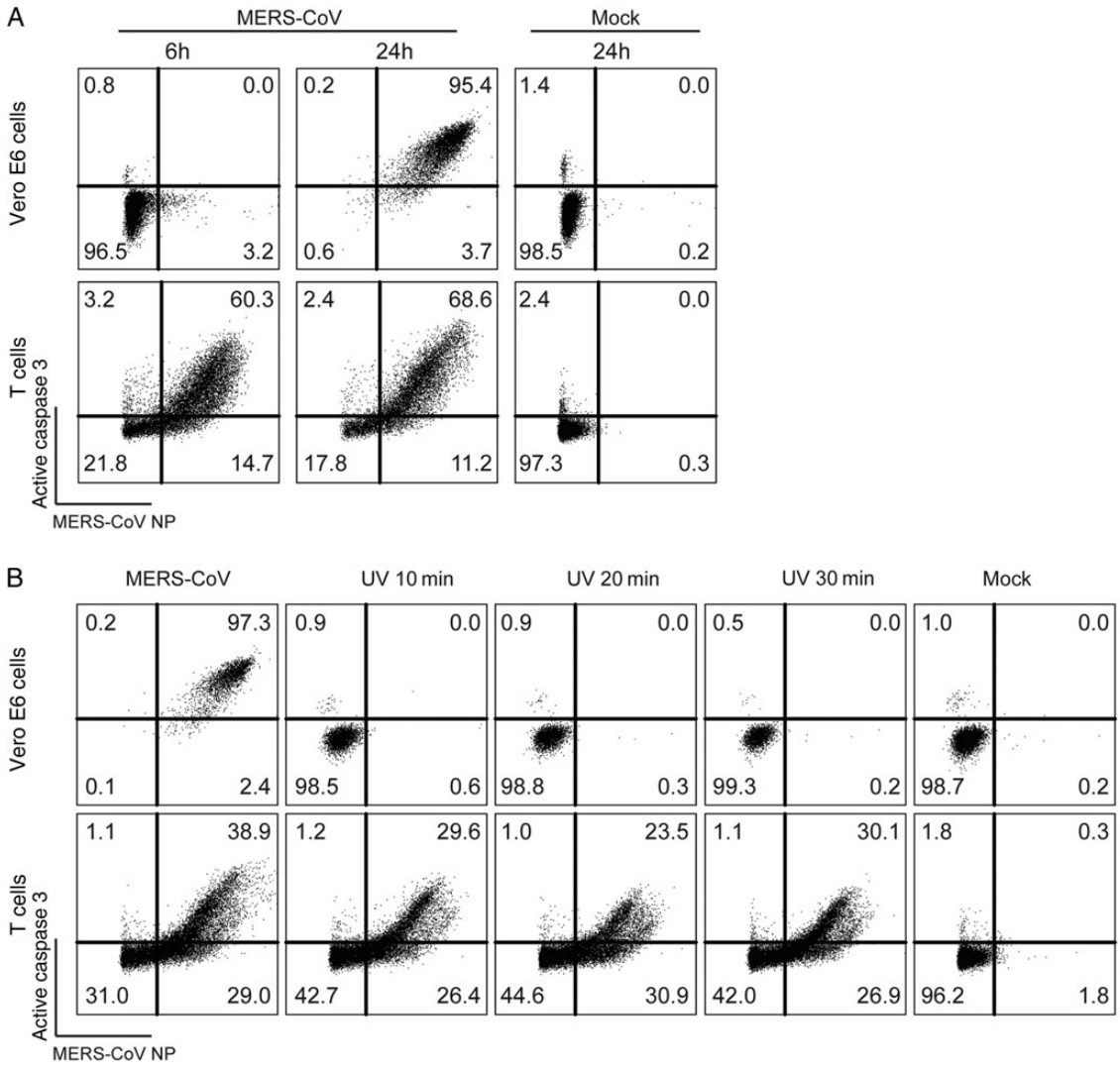

Figure 5. Middle East respiratory syndrome coronavirus (MERS-CoV)–induced caspase 3 activation in T cells occurs rapidly upon infection and is not inhibited by UV inactivation of the virus. *A*, T cells and Vero E6 cells were infected with MERS-CoV at 2 50% tissue culture infective doses ($TCID_{50}$) per cell. Cells were fixed at the indicated time points and immunolabeled for detection of MERS-CoV nucleoprotein (NP) and active caspase 3. *B*, T cells and Vero E6 cells were infected with MERS-CoV at 2 $TCID_{50}$ per cell. In parallel, equal volumes of UV-inactivated MERS-CoV were applied to Vero E6 cells and T cells. At 24 hours after infection, cells were harvested, fixed, and immunolabeled for detection of MERS-CoV NP and active caspase 3. The illustrated result was a representative of 2 independent experiments that showed similar results.

cells and compared the level of caspase 3 activation with that in infected T cells. Our data suggested that caspase 3 was also activated in Vero E6 cells, although the dynamic of activation was drastically different from that in T cells. Remarkably, at 6 hours after infection, only a subtle population of Vero E6 cells was infected by MERS-CoV, with no caspase 3 activation (Figure 5*A*). Intriguingly, at 24 hours after infection, essentially all Vero E6 cells were infected, and the vast majority of the infected cells were expressing activated caspase 3 (Figure 5*A*). On the other hand, a substantial number of T cells were infected at 6 hours after infection, with accompanying excessive caspase 3 activation. The level of infection and caspase 3 activation in T cells remained largely constant between 6 and 24 hours after infection (Figure 5*A*). Since Vero E6 cells are known to support robust MERS-CoV replication, we speculated that caspase 3 activation in Vero E6 cells was a result of virus replication. To test this hypothesis, we inoculated Vero E6 cells and T cells with UV-inactivated MERS-CoV. The replication capacity of MERS-CoV was completely abolished with 10 minutes of UV inactivation (Supplementary Figure 4). Strikingly, UV inactivation completely obliterated MERS-CoV infection and caspase 3 activation in Vero E6 cells (Figure 5*B*). In stark contrast, MERS-CoV entry and MERS-CoV–induced caspase 3 activation in T cells remained largely unaltered by UV inactivation (Figure 5*B*). NP staining with no cell permeabilization (Supplementary Figure 5*A*) or on ice before cell permeabilization (Supplementary Figure 5*B*) both picked up little to no signal, suggesting the detected MERS-CoV NP signal was indeed intracellular but not

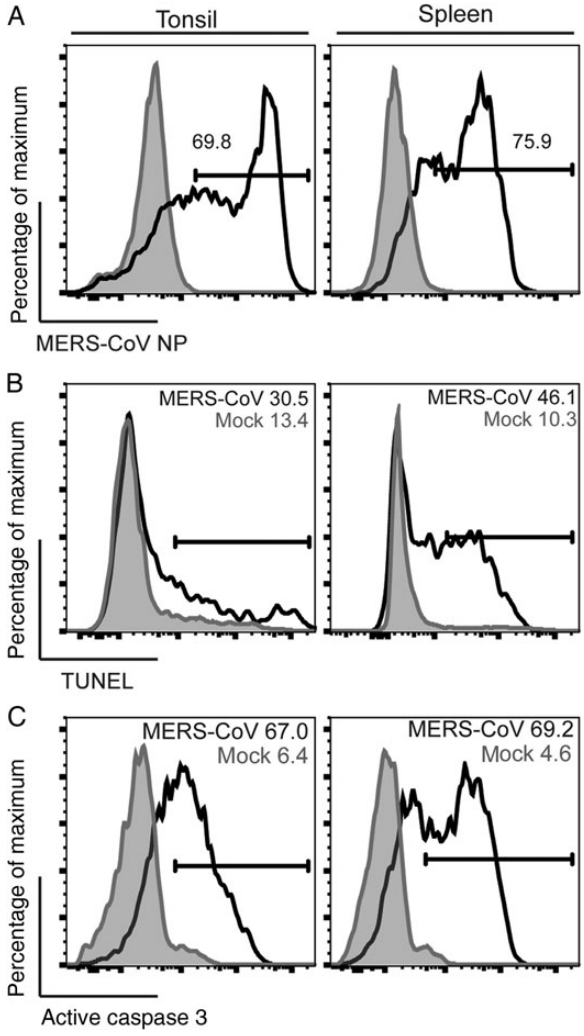

Figure 6. T cells in human lymphatic organs, including the spleen and the tonsil, are highly susceptible to Middle East respiratory syndrome coronavirus (MERS-CoV) and MERS-CoV–induced apoptosis. Disassociated human spleen and tonsil cells were infected with MERS-CoV at 2 50% tissue culture infective doses per cell. Cells were fixed at 24 hours after infection and assessed for MERS-CoV nucleoprotein (NP; *A*), terminal deoxynucleotidyl transferase dUTP nick end labeling activity (*B*), and active caspase 3 (*C*) among $CD3^+$ cells. The illustrated result was a representative of 2 independent experiments that showed similar results.

from surface-attached viruses. Together, these data illustrated intrinsic differences in the dynamics of MERS-CoV infection and MERS-CoV–induced caspase 3 activation in Vero E6 cells and T cells.

T Cells in Human Lymphatic Organs, Including the Tonsil and the Spleen, Are Highly Susceptible to MERS-CoV and MERS-CoV–Induced Apoptosis

Recent pathological studies detected the presence of viral RNA in the tonsil [30, 40, 41], lymph node [30, 40, 41], and spleen [30] of MERS-CoV–inoculated animals. To investigate whether T cells in these lymphoid organs are as susceptible to MERS-CoV infection as those in the peripheral blood, we inoculated disassociated cells from human spleen and tonsil with MERS-CoV and estimated the percentage of infected T cells by using flow cytometry. Remarkably, $CD3^+$ T cells from the spleen and tonsil were infected to a similar extent as T cells in the peripheral blood (Figure 6*A*). We further assessed the level of MERS-CoV–induced apoptosis in these cells. Our data suggested that the percentage of TUNEL-positive (Figure 6*B*) and active caspase 3–positive (Figure 6*C*) cells among MERS-CoV–infected $CD3^+$ T cells from the spleen and tonsil highly resembled that among the peripheral blood T cells. In this regard, we demonstrated that T cells in the human spleen and tonsil were highly susceptible to MERS-CoV infection and MERS-CoV–induced apoptosis.

MERS-CoV Infects $CD3^+$ T Cells in the Spleen of Common Marmosets

Our in vitro and ex vivo data have, so far, consistently demonstrated the high susceptibility of human T cells to MERS-CoV infection. We next used the common marmoset animal model [30, 31] to evaluate the involvement of T cells in MERS-CoV infection in vivo. Two male common marmosets (*Callithrix jacchus*; CM1 and CM2) were inoculated with 5×10^6 $TCID_{50}$ of MERS-CoV intratracheally. Upon necropsy of these infected animals, tissue samples were collected and analyzed for the presence of viral RNA. Notably, viral RNA was detected from the spleen tissues of both animals, with a viral gene to GAPDH ratio of 7.3×10^4 and 7.6×10^5 in CM1 and CM2, respectively (Supplementary Figure 6). Next, immunostaining was performed on paraformaldehyde-fixed and paraffin-embedded sections of spleen from the infected animals. Remarkably, MERS-CoV NP was readily detected in the spleen (Figure 7*D* and 7*G*). More importantly, MERS-CoV NP was detected in T cells, which was suggested by the colocalization between MERS-CoV NP and CD3 (Figure 7*D*–*I*). As a control, no MERS-CoV NP signal was detected when preimmune serum was used in place of MERS-CoV NP antibody (Figure 7*A*–*C*). Overall, we demonstrated the capacity of MERS-CoV to disseminate to the spleens of common marmosets and infect $CD3^+$ T cells therein, despite respiratory transmission of the pathogen.

DISCUSSION

T cells and T-cell responses play central roles in the pathogenesis of SARS [42, 43]. Currently, little is known about the virus-host interaction of MERS-CoV infection in T cells. In this study, we demonstrated that human T cells were highly susceptible to MERS-CoV infection and MERS-CoV–induced apoptosis while remaining impervious to SARS-CoV. Most importantly, we showed in a common marmoset model that MERS-CoV efficiently targeted the $CD3^+$ T cells in the spleen of infected animals. Together, our results suggested that its distinct capacity to invade T cells might contribute to the high pathogenicity of MERS-CoV.

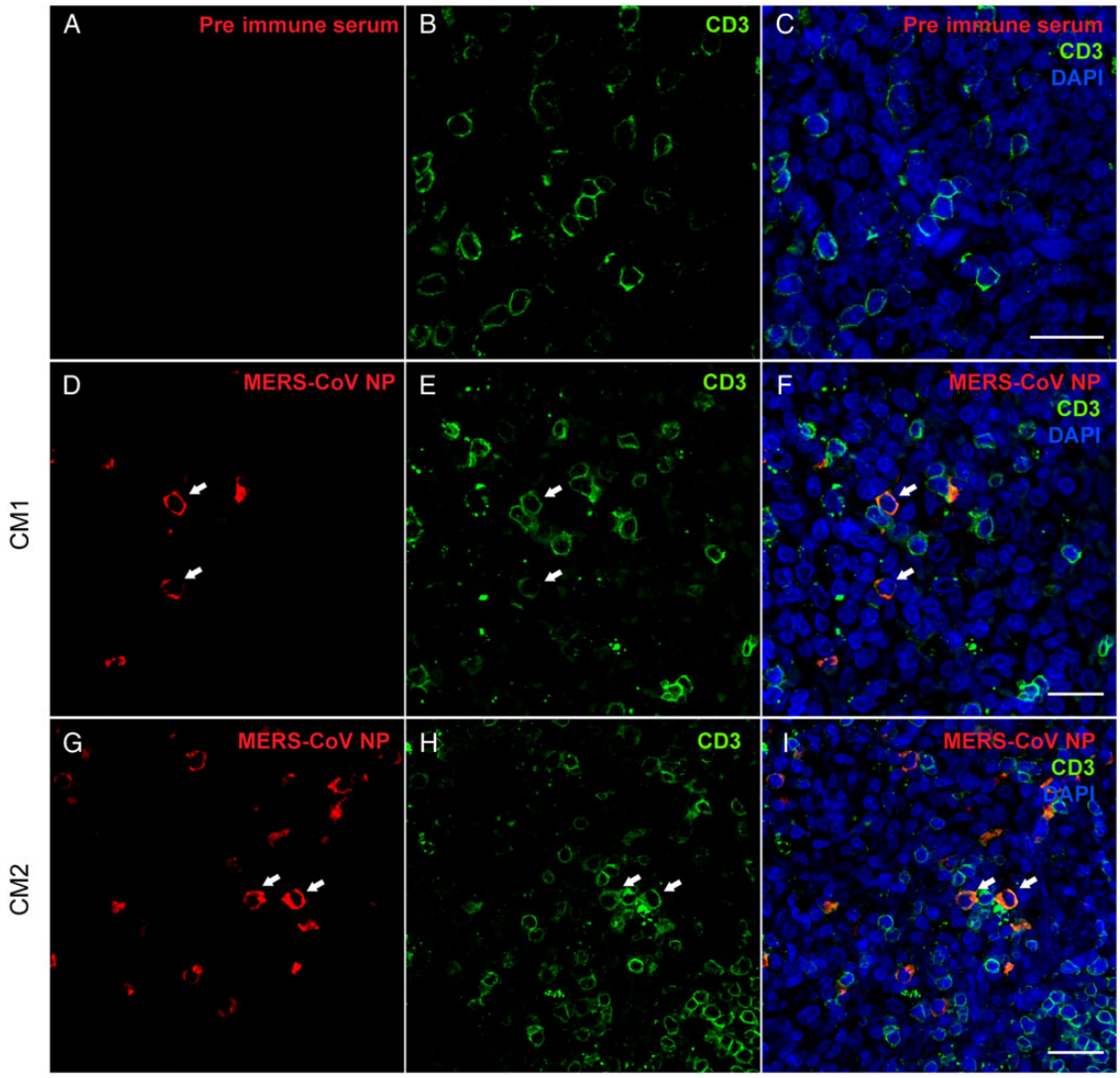

Figure 7. Middle East respiratory syndrome coronavirus (MERS-CoV) infects $CD3^+$ T cells in the spleen of infected common marmosets. Immunostaining was performed on paraformaldehyde-fixed and paraffin-embedded sections of spleen obtained on day 1 after virus challenge of animals. Colocalization between MERS-CoV nucleoprotein (NP; *D* and *G*) and CD3 (*E* and *H*) were detected in the spleen of the infected animals (arrows; *D–F* and *G–I*). CM1 and CM2 represent 2 individual common marmosets. MERS-CoV NP was not detected in the preimmune serum control (*A–C*). Bars represent 25 μm.

Viremia has been frequently reported in patients with SARS and those with MERS. Viral RNA was detected in the sera of SARS patients during the acute phase of infection [44, 45]. MERS-CoV RNA could be detected in the blood of infected patients for a prolonged period [46–48]. The viremia can be attributed to circulating free viral RNA that should be transient, free virion in blood or virus in infected cells. Remarkably, our current study demonstrated that MERS-CoV but not SARS-CoV efficiently infected T cells and induced substantial apoptosis in the infected cells. This discovery indicates that the viremia in patients with SARS and those with MERS may have different clinical significance. In particular, given the capacity of MERS-CoV to invade T cells, patients with MERS who develop viremia may have a more severe outcome. Of note, viremia is not the only route for MERS-CoV to infect T cells. T cells could be attracted to the infected lung under the action of chemoattractants and therefore be infected at the primary organ of MERS-CoV infection. Alternatively, dendritic cells, which we have previously shown to support robust MERS-CoV replication [22], can be infected, migrate to the draining lymph nodes, and transmit the virus to naive T cells during antigen presentation. Importantly, lymphopenia is a common hematological abnormality that has been frequently reported in SARS and MERS cases [7, 49]. It has been speculated that lymphopenia detected in SARS cases might be due to direct infection, tissue sequestration of lymphocytes, cytokine-mediated cell death, as well as suppression of bone marrow or thymus for T-cell generation. In this study, we demonstrated that MERS-CoV but not

SARS-CoV could directly infect T cells and induce apoptosis in the infected cells. Therefore, the underlying mechanism for SARS-CoV– and MERS-CoV–induced lymphopenia could be distinct. In particular, lymphopenia in MERS but not SARS cases could be a result of direct infection of T cells and infection-induced apoptosis. In addition to apoptosis, the dramatic depletion of surface DPP4 in T cells upon MERS-CoV infection may substantially disrupt the proliferation and cellular function of T cells. The mechanism and implication of MERS-CoV–directed DPP4 depletion in T cells deserve further investigation.

Multiple genes of SARS-CoV have been implicated in caspase induction [4]. We showed in the current study that MERS-CoV–induced apoptosis in T cells was accompanied by the activation of caspases 3, 8, and 9. The maturation of caspases 8 and 9 suggested that the extrinsic and intrinsic apoptosis pathways were triggered by MERS-CoV infection. Currently, the exact mechanism of MERS-CoV–induced caspase upregulation is unknown. However, since UV-inactivated MERS-CoV induced caspase 3 upregulation to an extent similar to that of untreated MERS-CoV, we postulate that the detected caspase upregulation is likely attributed to the structural components of MERS-CoV, including the E, M, S, and N proteins. Nevertheless, our data demonstrated that, while approximately 70% of MERS-CoV–infected T cells were expressing active caspase 3, a considerably lower percentage of infected T cells showed signs of caspase 8 or caspase 9 activation. Although the relationship of the quantity of initiator caspases (caspases 8 and 9) and execution caspase (caspase 3) is not linear, because they are catalyzed in a cascade, it is possible that other, yet-to-be-identified pathways are also involved in caspase 3 activation and in contributing to MERS-CoV–induced apoptosis in infected T cells. Remarkably, the dynamics of MERS-CoV infection and MERS-CoV–induced apoptosis in T cells were drastically different from findings in cell lines. We demonstrated that, whereas caspase 3 induction in cell lines was gradual and replication dependent, it was abrupt and replication-independent in T cells. This discrepancy is likely due to the difference in the efficiency of MERS-CoV entry of cell lines versus primary T cells, which may in turn be a result of differential surface DPP4 expression. In this regard, if virus-induced T-cell apoptosis is a pathogenic determinant of MERS, a novel treatment regimen such as one involving anti-apoptotic agents in addition to antivirals inhibiting virus replication may be considered to improve the outcomes of patients with MERS, as in the case of VX-765 for human immunodeficiency virus infection [50].

Recent animal studies have identified MERS-CoV RNA in the lymphoid organs of infected animals, including common marmosets [30], rhesus macaques [40], and dromedary camels [41]. However, owing to the lack of reports describing samples obtained from patients with MERS during autopsy, whether the virus could invade human lymphoid organs remained unknown. To this end, we inoculated disassociated human spleen and tonsil cells with MERS-CoV. Remarkably, $CD3^+$ T cells in the spleen and tonsil were highly susceptible to MERS-CoV infection and MERS-CoV–induced apoptosis. Intriguingly, T cells from these organs appeared to demonstrate a higher degree of infection and apoptosis upon MERS-CoV challenge. This suggested that T cells at different developmental stages might be differentially affected by MERS-CoV. Finally, we examined the spleen of MERS-CoV–infected common marmosets. Importantly, our data demonstrated that MERS-CoV could disseminate to the spleens of infected animals and infect their $CD3^+$ T cells. Collectively, our ex vivo and in vivo findings suggest that MERS-CoV can invade not only T cells in the peripheral blood, but also the large repertoire of T cells in lymphoid organs, which may result in a more severe immunopathology.

In summary, our study provided in vitro, ex vivo, and in vivo evidence for MERS-CoV infection of human T cells. We demonstrated that the infection is associated with apoptosis induction, which may provide a new target for effective therapeutic interventions.

Supplementary Data

Supplementary materials are available at *The Journal of Infectious Diseases* online (http://jid.oxfordjournals.org). Supplementary materials consist of data provided by the author that are published to benefit the reader. The posted materials are not copyedited. The contents of all supplementary data are the sole responsibility of the authors. Questions or messages regarding errors should be addressed to the author.

Notes

Acknowledgments. We thank Dr Birgitta Wong, Dr Jacky Lam, and the staff at the Core Facility, Li Ka Shing Faculty of Medicine, University of Hong Kong, for facilitation of the study.

Financial support. This work was partially supported by the Research Grants Council of the Hong Kong Special Administrative Region, China (Project No. T11/707/15), the Providence Foundation Limited in memory of the late Dr Lui Hac Minh, the University of Hong Kong Small Project Funding (201409176024), the Hong Kong Health and Medical Research Fund (14131392), Hong Kong Research Grants Council (N_HKU728/14), and the National Science and Technology Major Projects of Infectious Disease (2012ZX10004501-004).

Potential conflicts of interest. All authors: No reported conflicts. All authors have submitted the ICMJE Form for Disclosure of Potential Conflicts of Interest. Conflicts that the editors consider relevant to the content of the manuscript have been disclosed.

References

1. Zaki AM, van Boheemen S, Bestebroer TM, Osterhaus AD, Fouchier RA. Isolation of a novel coronavirus from a man with pneumonia in Saudi Arabia. N Engl J Med **2012**; 367:1814–20.
2. Bermingham A, Chand MA, Brown CS, et al. Severe respiratory illness caused by a novel coronavirus, in a patient transferred to the United Kingdom from the Middle East, September 2012. Euro Surveill **2012**; 17:20290.
3. Chan JF, Lau SK, To KK, Cheng VC, Woo PC, Yuen KY. Middle East respiratory syndrome coronavirus: another zoonotic betacoronavirus causing SARS-like disease. Clin Microbiol Rev **2015**; 28:465–522.
4. Cheng VC, Lau SK, Woo PC, Yuen KY. Severe acute respiratory syndrome coronavirus as an agent of emerging and reemerging infection. Clin Microbiol Rev **2007**; 20:660–94.
5. Peiris JS, Lai ST, Poon LL, et al. Coronavirus as a possible cause of severe acute respiratory syndrome. Lancet **2003**; 361:1319–25.
6. Chan JF, Li KS, To KK, Cheng VC, Chen H, Yuen KY. Is the discovery of the novel human betacoronavirus 2c EMC/2012 (HCoV-EMC) the beginning of another SARS-like pandemic? J Infect **2012**; 65:477–89.

7. Assiri A, Al-Tawfiq JA, Al-Rabeeah AA, et al. Epidemiological, demographic, and clinical characteristics of 47 cases of Middle East respiratory syndrome coronavirus disease from Saudi Arabia: a descriptive study. Lancet Infect Dis **2013**; 13:752–61.
8. Al-Abdallat MM, Payne DC, Alqasrawi S, et al. Hospital-associated outbreak of Middle East respiratory syndrome coronavirus: a serologic, epidemiologic, and clinical description. Clin Infect Dis **2014**; 59:1225–33.
9. Raj VS, Mou H, Smits SL, et al. Dipeptidyl peptidase 4 is a functional receptor for the emerging human coronavirus-EMC. Nature **2013**; 495:251–4.
10. Chan JF, To KK, Tse H, Jin DY, Yeun KY. Interspecies transmission and emergence of novel viruses: lessons from bats and birds. Trends Microbiol **2013**; 21:544–55.
11. Chan JF, Chan KH, Choi GK, et al. Differential cell line susceptibility to the emerging novel human betacoronavirus 2c EMC/2012: implications for disease pathogenesis and clinical manifestation. J Infect Dis **2013**; 207:1743–52.
12. Muller MA, Raj VS, Muth D, et al. Human coronavirus EMC does not require the SARS-coronavirus receptor and maintains broad replicative capability in mammalian cell lines. MBio **2012**; 3:e00515–12.
13. Eckerle I, Muller MA, Kallies S, Gotthardt DN, Drosten C. In-vitro renal epithelial cell infection reveals a viral kidney tropism as a potential mechanism for acute renal failure during Middle East Respiratory Syndrome (MERS) Coronavirus infection. Virol J **2013**; 10:359.
14. Zhou J, Chu H, Li C, et al. Active replication of Middle East respiratory syndrome coronavirus and aberrant induction of inflammatory cytokines and chemokines in human macrophages: implications for pathogenesis. J Infect Dis **2014**; 209: 1331–42.
15. Josset L, Menachery VD, Gralinski LE, et al. Cell host response to infection with novel human coronavirus EMC predicts potential antivirals and important differences with SARS coronavirus. MBio **2013**; 4:e00165-13.
16. Yang Y, Zhang L, Geng H, et al. The structural and accessory proteins M, ORF 4a, ORF 4b, and ORF 5 of Middle East respiratory syndrome coronavirus (MERS-CoV) are potent interferon antagonists. Protein Cell **2013**; 4:951–61.
17. Siu KL, Yeung ML, Kok KH, et al. Middle east respiratory syndrome coronavirus 4a protein is a double-stranded RNA-binding protein that suppresses PACT-induced activation of RIG-I and MDA5 in the innate antiviral response. J Virol **2014**; 88:4866–76.
18. Niemeyer D, Zillinger T, Muth D, et al. Middle East respiratory syndrome coronavirus accessory protein 4a is a type I interferon antagonist. J Virol **2013**; 87:12489–95.
19. Lau SK, Lau CC, Chan KH, et al. Delayed induction of proinflammatory cytokines and suppression of innate antiviral response by the novel Middle East respiratory syndrome coronavirus: implications for pathogenesis and treatment. J Gen Virol **2013**; 94:2679–90.
20. Yang X, Chen X, Bian G, et al. Proteolytic processing, deubiquitinase and interferon antagonist activities of Middle East respiratory syndrome coronavirus papain-like protease. J Gen Virol **2014**; 95:614–26.
21. Menachery VD, Eisfeld AJ, Schafer A, et al. Pathogenic influenza viruses and coronaviruses utilize similar and contrasting approaches to control interferon-stimulated gene responses. MBio **2014**; 5:e01174-14.
22. Chu H, Zhou J, Wong BH, et al. Productive replication of Middle East respiratory syndrome coronavirus in monocyte-derived dendritic cells modulates innate immune response. Virology **2014**; 454–455:197–205.
23. Faure E, Poissy J, Goffard A, et al. Distinct immune response in two MERS-CoV-infected patients: can we go from bench to bedside? PLoS One **2014**; 9:e88716.
24. Torimoto Y, Dang NH, Vivier E, Tanaka T, Schlossman SF, Morimoto C. Coassociation of CD26 (dipeptidyl peptidase IV) with CD45 on the surface of human T lymphocytes. J Immunol **1991**; 147:2514–7.
25. Ishii T, Ohnuma K, Murakami A, et al. CD26-mediated signaling for T cell activation occurs in lipid rafts through its association with CD45RO. Proc Natl Acad Sci U S A **2001**; 98:12138–43.
26. Tanaka T, Kameoka J, Yaron A, Schlossman SF, Morimoto C. The costimulatory activity of the CD26 antigen requires dipeptidyl peptidase IV enzymatic activity. Proc Natl Acad Sci U S A **1993**; 90:4586–90.
27. Zhao J, Li K, Wohlford-Lenane C, et al. Rapid generation of a mouse model for Middle East respiratory syndrome. Proc Natl Acad Sci U S A **2014**; 111:4970–5.
28. Chu H, Wang JJ, Qi M, et al. Tetherin/BST-2 is essential for the formation of the intracellular virus-containing compartment in HIV-infected macrophages. Cell Host Microbe **2012**; 12:360–72.
29. Yao Y, Bao L, Deng W, et al. An animal model of MERS produced by infection of rhesus macaques with MERS coronavirus. J Infect Dis **2014**; 209:236–42.
30. Falzarano D, de Wit E, Feldmann F, et al. Infection with MERS-CoV causes lethal pneumonia in the common marmoset. PLoS Pathog **2014**; 10:e1004250.
31. Chan JF, Yao Y, Yeung ML, et al. Treatment with lopinavir/ritonavir or interferon-β1b improves outcome of MERS-CoV infection in a non-human primate model of common marmoset. J Infect Dis **2015**; 212:1904–13.
32. Che XY, Qiu LW, Pan YX, et al. Sensitive and specific monoclonal antibody-based capture enzyme immunoassay for detection of nucleocapsid antigen in sera from patients with severe acute respiratory syndrome. J Clin Microbiol **2004**; 42:2629–35.
33. Chan JF, Choi GK, Tsang AK, et al. Development and evaluation of novel real-time reverse transcription-PCR assays with locked nucleic acid probes targeting leader sequences of human-pathogenic coronaviruses. J Clin Microbiol **2015**; 53:2722–6.
34. Chan JF, Chan KH, Kao RY, et al. Broad-spectrum antivirals for the emerging Middle East respiratory syndrome coronavirus. J Infect **2013**; 67:606–16.
35. Tao X, Hill TE, Morimoto C, Peters CJ, Ksiazek TG, Tseng CT. Bilateral entry and release of Middle East respiratory syndrome coronavirus induces profound apoptosis of human bronchial epithelial cells. J Virol **2013**; 87:9953–8.
36. de Wilde AH, Raj VS, Oudshoorn D, et al. MERS-coronavirus replication induces severe in vitro cytopathology and is strongly inhibited by cyclosporin A or interferon-alpha treatment. J Gen Virol **2013**; 94:1749–60.
37. Gavrieli Y, Sherman Y, Ben-Sasson SA. Identification of programmed cell death in situ via specific labeling of nuclear DNA fragmentation. J Cell Biol **1992**; 119:493–501.
38. Elmore S. Apoptosis: a review of programmed cell death. Toxicol Pathol **2007**; 35:495–516.
39. Slee EA, Adrain C, Martin SJ. Executioner caspase-3, -6, and -7 perform distinct, non-redundant roles during the demolition phase of apoptosis. J Biol Chem **2001**; 276:7320–6.
40. de Wit E, Rasmussen AL, Falzarano D, et al. Middle East respiratory syndrome coronavirus (MERS-CoV) causes transient lower respiratory tract infection in rhesus macaques. Proc Natl Acad Sci U S A **2013**; 110:16598–603.
41. Adney DR, van Doremalen N, Brown VR, et al. Replication and shedding of MERS-CoV in upper respiratory tract of inoculated dromedary camels. Emerg Infect Dis **2014**; 20:1999–2005.
42. Zhao J, Zhao J, Van Rooijen N, Perlman S. Evasion by stealth: inefficient immune activation underlies poor T cell response and severe disease in SARS-CoV-infected mice. PLoS Pathog **2009**; 5:e1000636.
43. Zhao J, Zhao J, Perlman S. T cell responses are required for protection from clinical disease and for virus clearance in severe acute respiratory syndrome coronavirus-infected mice. J Virol **2010**; 84:9318–25.
44. Drosten C, Gunther S, Preiser W, et al. Identification of a novel coronavirus in patients with severe acute respiratory syndrome. N Engl J Med **2003**; 348:1967–76.
45. Grant PR, Garson JA, Tedder RS, Chan PK, Tam JS, Sung JJ. Detection of SARS coronavirus in plasma by real-time RT-PCR. N Engl J Med **2003**; 349:2468–9.
46. Poissy J, Goffard A, Parmentier-Decrucq E, et al. Kinetics and pattern of viral excretion in biological specimens of two MERS-CoV cases. J Clin Virol **2014**; 61:275–8.
47. Kapoor M, Pringle K, Kumar A, et al. Clinical and laboratory findings of the first imported case of Middle East respiratory syndrome coronavirus to the United States. Clin Infect Dis **2014**; 59:1511–8.
48. Kraaij-Dirkzwager M, Timen A, Dirksen K, et al. Middle East respiratory syndrome coronavirus (MERS-CoV) infections in two returning travellers in the Netherlands, May 2014. Euro Surveill **2014**; 19:pii:20817.
49. He Z, Zhao C, Dong Q, et al. Effects of severe acute respiratory syndrome (SARS) coronavirus infection on peripheral blood lymphocytes and their subsets. Int J Infect Dis **2005**; 9:323–30.
50. Doitsh G, Galloway NL, Geng X, et al. Cell death by pyroptosis drives CD4 T-cell depletion in HIV-1 infection. Nature **2014**; 505:509–14.